

Robust integrated optofluidic-ring-resonator dye lasers

Yuze Sun, Jonathan D. Suter, and Xudong Fan*

Department of Biological Engineering, University of Missouri, 240D Bond Life Sciences Center,
1201 East Rollins Street, Columbia, Missouri 65211, USA

*Corresponding author: fanxud@missouri.edu

Received January 13, 2009; accepted February 14, 2009;
posted March 4, 2009 (Doc. ID 106323); published March 25, 2009

We demonstrate a robust optofluidic dye laser that integrates fluidics with a high Q -factor ring resonator. In this optofluidic laser the ring resonator is formed by an optical fiber fused on the inner surface of a glass capillary serving as a fluidic channel. Laser oscillation is achieved with a threshold of $7 \mu\text{J}/\text{mm}^2$ per pulse. Furthermore, the laser emission can be directionally outcoupled through a fiber prism for easy and efficient light delivery. © 2009 Optical Society of America

OCS codes: 230.5750, 170.4520, 140.0140, 140.2050, 140.3325.

Optofluidic dye lasers are an emerging technology that combines advantages of fluidic control provided by microfluidics with the adaptive nature of dye lasers [1,2]. They have broad applications in micrototal analysis systems for biological–chemical sensing and in development of compact, tunable, multicolored light sources. In current optofluidic lasers, the optical feedback is provided by distributed feedback gratings [3–6] or Fabry–Perot-type resonators [7–10] embedded in polydimethylsiloxane (PDMS) chips. Single-mode operation [3], tunable output [5,6], and multi-color emission [9] have been demonstrated. However, owing to the small Young’s modulus of PDMS, PDMS-based optofluidic dye lasers suffer from low mechanical strength and are easy to deform under pressure. As a consequence, fast circulation of dye solution in a fluidic channel, which is highly desirable in achieving cw laser operation [2], cannot be sustained. Additionally, the Q factor of the above lasers is on the order of 10^3 , resulting in a relatively high lasing threshold.

Optical ring resonators, such as microdroplets [11,12], microspheres [13,14], microcylinders [15], microcapillaries [16–20], microfiber knots [21], and ring-shaped waveguides formed on a PDMS substrate [22], are also commonly used in optofluidic dye lasers. In those ring resonators, whispering gallery modes (WGMs) of high Q factors ($>10^6$) circulate along the ring-resonator surface, providing an excellent optical feedback for low-threshold lasing. However, a few significant drawbacks still exist in current optofluidic ring-resonator (OFRR) lasers, including ineffective integration with microfluidics (such as in microspheres [13,14] and microfiber knots [21]), difficulty in mass producing and integrating into practical and functional optical devices (such as in microdroplets [11] and microspheres [13,14]), lack of efficient directional outcoupling (such as in microdroplets [11], microcapillaries [16,17], and microcylinders [15]), and relatively weak mechanical strength (such as in microcapillaries [18,19], microfiber knots [21], and PDMS-based ring resonators [22]).

To address those issues, in this work we report the design and performance of a new type of OFRR dye laser. As illustrated in Figs. 1(a) and 1(b), a microcyl-

inder ring resonator is fused onto the inner surface of a capillary. When a solvent with a refractive index (RI) lower than the microcylinder is used, the microcylinder forms a ring resonator and supports WGMs of relatively high Q factors [Fig. 1(c)]. This OFRR dye laser offers a few distinctive advantages. First, the outer capillary provides an efficient fluidic channel for the ring resonator inside. Second, both ring resonator and fluidics are highly robust to accommodate a high flow rate of the dye solution, a critical feature to reduce the thermal effect in dye lasers and to achieve microfluidic cw dye lasers. Third, when properly fabricated, the OFRR can potentially have high Q factors, yielding a low lasing threshold. Fourth, the lasing emission can be directionally coupled out through a fiber prism in contact with the outer capillary wall. Fifth, the fabrication process is simple and cost effective, and is compatible with commercial fiber drawing technology. Furthermore, the capillary provides an isolated environment so that an array of

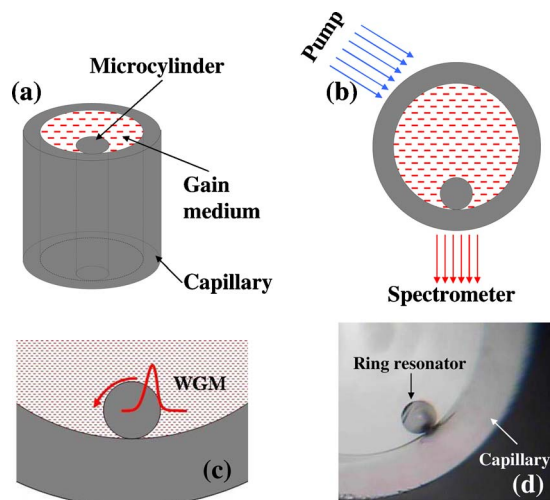


Fig. 1. (Color online) Conceptual illustrations of OFRR dye lasers: (a) side view, (b) cross-sectional view, (c) enlarged cross-sectional view of the OFRR, and (d) image of the fabricated OFRR dye laser. OFRR diameter = $125 \mu\text{m}$. Capillary inner diameter = $900 \mu\text{m}$ and outer diameter = $1200 \mu\text{m}$.

OFRR lasers can be packaged in a polymer without affecting their performance [20].

To fabricate this OFRR system, a segment (~ 5 cm) of an optical fiber without the polymer coating is inserted into a fused-silica capillary and then fused with the capillary inner wall by CO_2 laser irradiation. The CO_2 laser power is optimized to minimize the contact area between the microcylinder and capillary, thus retaining the high- Q factors of the ring resonator while providing strong mechanical strength [see Fig. 1(d)].

Figure 1(b) depicts the experimental setup. We use 1 mM R6G dye in methanol ($n=1.329$) as the gain medium, and it is flowed through the capillary at a flow rate of 0.7 mL/min. A pulsed optical parametric oscillator (532 nm and 5 ns pulse width) is used to illuminate a 3 mm portion of the OFRR. The dye emission is collected through free space and sent to a spectrometer (spectral resolution=0.12 nm).

A typical WGM lasing spectrum from the OFRR system is shown in Fig. 2(a). The periodic peaks emerge above the fluorescence baseline between 565 and 583 nm with the central wavelength at 573 nm. The free spectral range (FSR) is measured to be 0.566 nm, in agreement with the 125 μm diameter of the fiber. The WGM spectrum of another optofluidic laser system fabricated by the same method is given in Fig. 2(b) with an FSR of 0.53 nm, indicative of a slight size variation ($\sim 5\%$) in fabrication. The central wavelength moves to 565 nm, suggesting a Q factor lower than that in Fig. 2(a) [19], which is attributed to a higher leakage of the WGM into the capillary wall through the fused contact area.

The FSR in both Figs. 2(a) and 2(b) suggests that the laser oscillation comes from the ring resonator instead of the capillary wall as reported in earlier studies [15,17]. To further verify the origin of the optical feedback in the laser emission, a capillary of the same dimension in the absence of the ring resonator is filled with the same concentration of R6G and is pumped at the energy level far above the lasing threshold. No lasing oscillation is observed, consistent with previous results [16].

Figure 3(a) plots the lasing peak intensity as a function of the pump intensity. Below the lasing threshold, only broad R6G emission is observed [Fig. 2(b)]. With the increased pump power, the laser peaks emerge at 565 nm. The lasing threshold is approximately $7 \mu\text{J}/\text{mm}^2$ per pulse. Although the lasing threshold is much higher than the best reported

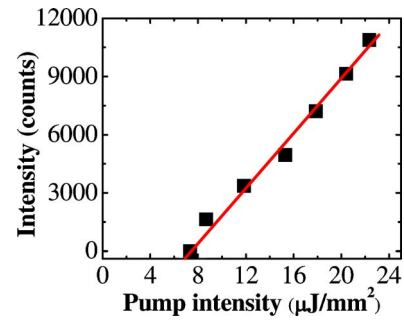


Fig. 3. (Color online) Intensity of the lasing emission peak at 565 nm in Fig. 2(b) versus the pump intensity.

silica-based OFRR dye lasers [19], it is on par with many PDMS-based optofluidic dye lasers [3,5,8].

The intrinsic Q factor or the empty-cavity Q factor (in the absence of dye) of the OFRR system, Q_0 , can be deduced from the spectral position of the laser emission peak [15,19]. Since the gain medium overlaps only with the evanescent field of the WGM, the laser emission spectrum is determined by ηQ_0 , where η is the fraction of the WGM in the evanescent field. According to Fig. 2(a), the peak of the laser emission is around 573 nm, which corresponds to a ηQ_0 value of 4×10^4 based on the study reported in [15,19]. Considering that η is typically a few percent [15], Q_0 is estimated to be around 10^6 . Likewise, for the ring resonator in Fig. 2(b), Q_0 of 10^5 is deduced. Although the Q factor is higher than that in the PDMS-based cavity, it is 1 to 2 orders of magnitude lower than that in a stand-alone microcylinder ring resonator, which is caused mainly by the loss to the capillary wall at the point of contact.

The ability to directionally couple the laser emission out is highly desirable in many practical applications. Previously, the directional outcoupling of the laser emission from a ring resonator via the evanescent coupling was demonstrated by placing a fiber taper, fiber prism, or waveguide in contact with the ring resonator [18–20]. However, for a microcylinder ring resonator suspended in the center of a capillary [15], a structure similar to the OFRR laser system reported in this Letter, direct contact between the ring resonator and a fiber or waveguide is challenging. Consequently, the laser emission can be coupled out only by collecting the laser scattering in free space. For our OFRR laser, direct evanescent coupling from the ring resonator also seems to be impossible, as it is shielded by a 150- μm -thick capillary wall. However,

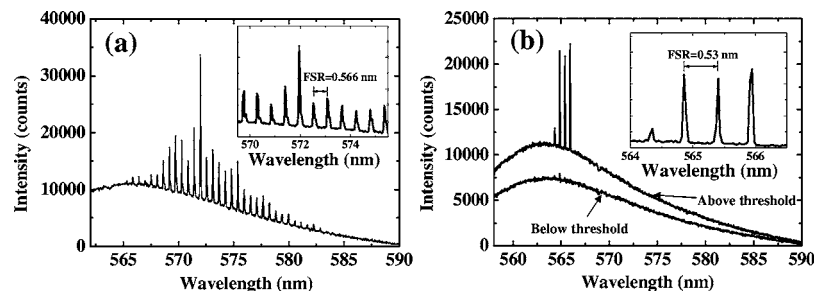


Fig. 2. WGM lasing spectra of two OFRR R6G lasers collected in free space. Insets, laser spectra with the fluorescence background removed.

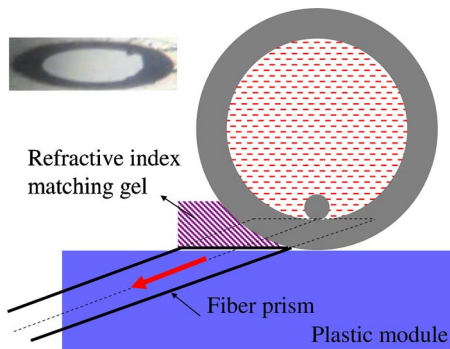


Fig. 4. (Color online) Fiber prism outcoupling setup. The dashed line profile indicates the virtual extension of the fiber prism. Inset, image of the fiber prism surface.

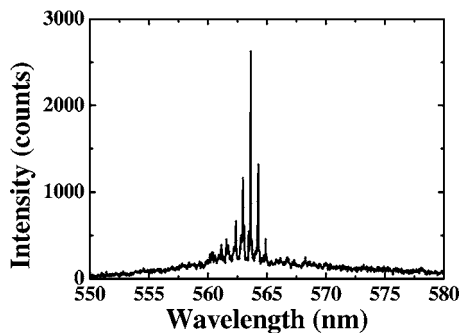


Fig. 5. Directional outcoupling of the OFRR dye laser through a fiber prism.

we will show the feasibility of outcoupling the laser light through a fiber prism via the evanescent coupling. As illustrated in Fig. 4, an SMF-28 fiber is first glued in a plastic module and then angle polished at 15° at one of its ends [20]. Then the fiber prism is placed below the ring resonator, and the gap between the fiber prism surface and the capillary is filled with RI matching gel ($n=1.45$). Through this design, the fiber prism surface can be effectively extended to the surface right below the ring resonator (dashed lines in Fig. 4). In the experiment, the whole OFRR system is slightly shifted horizontally to compensate for the displacement of the fiber prism surface.

Figure 5 shows the laser emission coupled out of the fiber prism. Most of the strong fluorescence baseline is rejected compared to the free-space collection method. Ideally only the WGM laser emission is phase matched and therefore can be coupled into the fiber prism. Since the long axis of the fiber prism core is only $30\ \mu\text{m}$ long, the coupling efficiency drops significantly with only slight horizontal misalignment, further confirming that the laser emission in Fig. 5 is not from the laser scattering but the directional coupling.

In summary, we have demonstrated a robust OFRR dye laser that is integrated with capillary-based fluidics and can potentially be mass produced in a simple and cost-effective manner. A lasing threshold

of $7\ \mu\text{J}/\text{mm}^2$ per pulse is achieved, and the laser emission can be outcoupled directionally through a fiber prism. Future work will be focused on the fabrication method to fully take advantage of the intrinsic high Q factors of the ring resonator for an even lower lasing threshold. Additionally, microcylinders of higher RI materials such as sapphire and chalcogenides can be used to reduce the loss to the capillary wall and to impart more flexibility to dye and solvent selection. Tuning of the laser wavelength and single-mode lasing will also be pursued.

The authors acknowledge support from the National Science Foundation (NSF) (CBET-0747398).

References

1. C. Monat, P. Domachuk, and B. J. Eggleton, *Nat. Photonics* **1**, 106 (2007).
2. Z. Li and D. Psaltis, *Microfluid. Nanofluid.* **4**, 145 (2008).
3. Z. Li, Z. Zhang, T. Emery, A. Scherer, and D. Psaltis, *Opt. Express* **14**, 696 (2006).
4. S. Balslev and A. Kristensen, *Opt. Express* **13**, 344 (2005).
5. M. Gersborg-Hansen and A. Kristensen, *Opt. Express* **15**, 137 (2007).
6. Z. Li, Z. Zhang, A. Scherer, and D. Psaltis, *Opt. Express* **14**, 10494 (2006).
7. B. Helbo, A. Kristensen, and A. Menon, *J. Micromech. Microeng.* **13**, 307 (2003).
8. D. V. Vezenov, B. T. Mayers, R. S. Conroy, G. M. Whitesides, P. T. Snee, Y. Chan, D. G. Nocera, and M. G. Bawendi, *J. Am. Chem. Soc.* **127**, 8952 (2005).
9. Q. Kou, I. Yesilyurt, and Y. Chen, *Appl. Phys. Lett.* **88**, 091101 (2006).
10. J. C. Galas, J. Torres, M. Belotti, Q. Kou, and Y. Chen, *Appl. Phys. Lett.* **86**, 264101 (2005).
11. S.-X. Qian, J. B. Snow, H.-M. Tzeng, and R. K. Chang, *Science* **231**, 486 (1986).
12. M. Tanyeri, R. Perron, and I. M. Kennedy, *Opt. Lett.* **32**, 2529 (2007).
13. H. Fujiwara and K. Sasaki, *Jpn. J. Appl. Phys. Part 1* **38**, 5101 (1999).
14. K. An and H.-J. Moon, *J. Phys. Soc. Jpn.* **72**, 773 (2003).
15. H.-J. Moon, Y.-T. Chough, and K. An, *Phys. Rev. Lett.* **85**, 3161 (2000).
16. J. C. Knight, H. S. T. Driver, R. J. Hutcheon, and G. N. Robertson, *Opt. Lett.* **17**, 1280 (1992).
17. H.-J. Moon and K. An, *Appl. Phys. Lett.* **80**, 3250 (2002).
18. S. I. Shopova, H. Zhu, X. Fan, and P. Zhang, *Appl. Phys. Lett.* **90**, 221101 (2007).
19. S. Lacey, I. M. White, Y. Sun, S. I. Shopova, J. M. Cupps, P. Zhang, and X. Fan, *Opt. Express* **15**, 15523 (2007).
20. J. D. Suter, Y. Sun, D. J. Howard, J. Viator, and X. Fan, *Opt. Express* **16**, 10248 (2008).
21. X. Jiang, Q. Song, L. Xu, J. Fu, and L. Tong, *Appl. Phys. Lett.* **90**, 233501 (2007).
22. Z. Li, Z. Zhang, A. Scherer, and D. Psaltis, in *LEOS Summer Topical Meetings* (2007), p. 70.